Coupling Numerators and Input–Output Pairing in Square Control Systems

R. A. Hess*
University of California, Davis, Davis, California 95616

Introduction

THE use of coupling numerators as a analysis/synthesis tool for frequency-domain control system design is well established.[1] Of particular interest is their use in approximating "effective" plant dynamics between a particular plant input and output pair when remaining response variables are assumed to be tightly constrained by feedback.[2] After simplifying of the calculation of coupling numerators, their use in the selection of appropriate pairings of plant inputs and outputs for square feedback designs can be demonstrated. The effect of plant transmission zeros on individual effective plant transfer functions when other response variables are tightly constrained follows naturally from this approach.

To begin this discussion, consider the state-space formulation for a linear system:

$$\dot{x}(t) = Ax(t) + Bu(t), \qquad y(t) = Cx(t) + Du(t) \tag{1}$$

The plant transfer function matrix $P(s)$ can be introduced as

$$y(s) = [C(sI - A)^{-1}B + D]u(s) = P(s)u(s) \tag{2}$$

An alternative means of describing system input–output behavior in the Laplace domain can be given as

$$E(s)y(s) = u(s) = Iu(s) \tag{3}$$

or

$$y(s) = E^{-1}(s)u(s) \tag{4}$$

When it is assumed that $P^{-1}(s)$ exists, Eqs. (2) and (3) yield

$$E(s) = P^{-1}(s) = [P_{\text{adj}}]^T \big/ \det P(s) \tag{5}$$

Coupling Numerators

Equation (3) leads to the definition of coupling numerators as described in Ref. 1. In Ref. 1, the vector $y(s)$ represents the transformed state variable vector, whereas here it represents the transformed output vector. The matrix algebra remains unchanged, however, and this formulation leads to a particularly simple form for the coupling numerators. For example, a coupling numerator of order 1 between two response variables $y_1(s)$ and $y_2(s)$ and two control inputs $u_1(s)$ and $u_2(s)$ in a 2×2 system can be given simply as

$$N_{u_1u_2}^{y_1y_2}(s) = \begin{vmatrix} 1 & 0 \\ 0 & 1 \end{vmatrix} = 1.0 \tag{6}$$

Note that the coupling numerator of Eq. (6) has no polynomials in its elements and is considerably simpler than those encountered when the system description of Ref. 1 is used. For the purposes of exposition, the following discussion and example will concentrate on 2×2 systems. It should be emphasized that extension to $n \times n$ square systems is straightforward.

Received 15 July 2002; revision received 1 August 2002; accepted for publication 11 November 2002.

*Professor and Vice Chairman, Department of Mechanical and Aeronautical Engineering. Associate Fellow AIAA.

Sequential Loop Closure in a Square Systems

Consider the 2×2 square control system of Fig. 1. The matrix $K(s)$ can be a static control distribution matrix or contain dynamic elements that serve as pre-compenators, for example, to decouple approximately the plant.[3] At this juncture, $K(s)$ is the identity matrix and $u_1(s) \equiv v_1(s)$ and $u_2(s) \equiv v_2(s)$. Here two linear compensation elements $G_1(s)$ and $G_2(s)$ are shown, that is, the compensation matrix is diagonal. It will be assumed that the design in question is a sequential loop-closure procedure and that $G_1(s)$ has been obtained by loop shaping with the second loop open. To design $G_2(s)$, a model of the effective plant with $G_1(s)$ in place is sought. Reference 1 shows that

$$\left.\frac{y_2}{u_2}(s)\right|_{y_1 \to u_1} = \frac{y_2}{u_2}(s) \cdot \frac{1 + G_1(s)\left(N_{u_2u_1}^{y_2y_1} \big/ N_{u_2}^{y_2}\right)}{1 + G_1(s)(y_1/u_1)(s)} \tag{7}$$

where the notation on the left-hand side of Eq. (7) means that the first loop has been closed with a feedback of y_1 through the compensation G_1 to provide u_1. For "tightly constrained" control in the first control loop, consider $|G_1(s)| \gg 1$. Thus,

$$\left.\frac{y_2}{u_2}(s)\right|_{y_1 \to u_1} \cong \frac{y_2}{u_2}(s) \cdot \frac{G_1(s)\left(N_{u_2u_1}^{y_2y_1} \big/ N_{u_2}^{y_2}\right)}{G_1(s)(y_1/u_1)(s)} = \frac{y_2}{u_2}(s) \cdot \frac{N_{u_2u_1}^{y_2y_1} \big/ N_{u_2}^{y_2}}{(y_1/u_1)(s)} \tag{8}$$

Note that terms such as

$$(y_1/u_1)(s) = P_{11}(s), \qquad (y_2/u_2)(s) = P_{22}(s), \ldots \tag{9}$$

Following the format of Ref. 1, the coupling numerator of order 0 is obtained as

$$N_{u_2}^{y_2} = \begin{vmatrix} e_{11}(s) & 0 \\ e_{21}(s) & 1 \end{vmatrix} = e_{11}(s) \tag{10}$$

However, from Eq. (5),

$$e_{11}(s) = \frac{P_{22}(s)}{\det P(s)} \tag{11}$$

Thus, with Eqs. (6–11), Eq. (8) becomes

$$\left.\frac{y_2}{u_2}(s)\right|_{y_1 \to u_1} \cong \frac{P_{22}(s)}{P_{11}(s)} \frac{\det P(s)}{P_{22}(s)} = \frac{\det P(s)}{P_{11}(s)} \tag{12}$$

Transmission zeros of the square plant of Fig. 1 are defined as zeros of $\det P(s)$ (Ref. 4) Equation (12) demonstrates that transmission zeros of a plant will appear as zeros of effective plant transfer functions when previous loop(s) are tightly constrained. Here tightly constrained means that previous loops are closed with arbitrarily high bandwidths. This, in turn, means that if there are transmission zeros in the right-half plane (RHP), the bandwidth of subsequent loop closures will be limited to values considerably smaller than the magnitude of these RHP zeros. Whereas the importance of transmission zeros has been emphasized in state-space control system synthesis techniques, their role in classical, frequency-domain designs is not often discussed.

The square system of Fig. 1 with $K(s)$ as the identity matrix implies plant input–output pairing, that is, $u_1(s)$ is used to control $y_1(s)$ and $u_2(s)$ is used to control $y_2(s)$. It can be easily shown that the use of a matrix $K(s)$ differing from the identity matrix

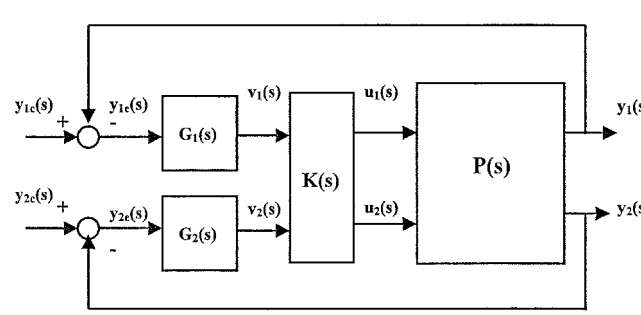

Fig. 1 Control system: 2×2 square.

will still result in transmission zeros appearing in effective plant transfer functions. From Fig. 1, one sees new pseudocontrols $v_1(s)$ and $v_2(s)$ serving as inputs to the $K(s)$. The pseudocontrols are then distributed to $u_1(s)$ and $u_2(s)$ through $K(s)$. One may now define a new plant matrix $P'(s)$ as

$$P'(s) = P(s)K(s) \tag{13}$$

Again, assume that the first loop is closed as before with a new $G_1(s)$ with $|G_1(s)| \gg 1$. The effective plant for the second loop closure can be obtained from Eq. (12) as

$$\left.\frac{y_2}{v_2}(s)\right|_{y_1 \to v_1} \cong \frac{\det P'(s)}{P'_{11}(s)} = \frac{\det P(s) \cdot \det K(s)}{P'_{11}(s)} \tag{14}$$

Equation (14) clearly indicates that, with the first loop tightly constrained, the second loop will again exhibit the transmission zeros of the plant $P(s)$.

In many applications, the number of plant inputs exceeds the number of plant outputs. In such cases, both $P(s)$ and $K(s)$ are rectangular. The approach just outlined remains valid. One merely replaces $P(s)$ with $P(s)K(s)$ and considers the $K(s)$ of Fig. 1 as the identity matrix. However, note that the result on the far right-hand side of Eq. (14) is no longer valid because the determinants of $P(s)$ and $K(s)$ are no longer defined. The pertinent transmission zeros would be those of $P(s)K(s)$.

Input–Output Pairing

The coupling numerator approach can be used to provide guidance in selecting input–output pairs for square systems. Assume that it is desired to change the pairing of input–output variables and redraw Fig. 1 to allow $u_1(s)$ to control $y_2(s)$ and $u_2(s)$ to control $y_1(s)$. Similar to Eqs. (7) and (8), the effective plant transfer function with $y_i(s)$ tightly constrained by $u_j(s)$, $i \neq j$, would be

$$\left.\frac{y_i}{u_j}(s)\right|_{y_j \to u_i} \cong \frac{y_i}{u_j}(s) \cdot \frac{G_i(s)\left(N^{y_2 y_1}_{u_1 u_2} \big/ N^{y_i}_{u_j}\right)}{G_i(s)(y_j/u_i)(s)}$$

$$= \frac{y_i}{u_j}(s) \cdot \frac{N^{y_2 y_1}_{u_1 u_2} \big/ N^{y_i}_{u_j}}{(y_j/u_i)(s)} = -\frac{y_i}{u_j} \cdot \frac{N^{y_2 y_1}_{u_2 u_1} \big/ N^{y_i}_{u_j}}{y_j/u_i} \tag{15}$$

and, finally,

$$\left.\frac{y_i}{u_j}(s)\right|_{y_j \to u_i} \cong -\frac{P_{ij}(s)}{P_{ji}(s)} \frac{\det P(s)}{[-P_{ij}(s)]} = \frac{\det P(s)}{P_{ji}(s)} \tag{16}$$

As will be demonstrated in the example of the next section, the resulting transfer functions defined by Eqs. (7) and (16) can provide guidance as to the selection of acceptable input–output pairs. Here "acceptable" includes a requirement for closed-loop stability when any loop is cut at the input to $K(s)$. Input–output pairing is an important step in a number of control system synthesis techniques such as quantitiative feedback theory (QFT)[5] and sliding mode control (SMC) using feedback linearization.[6] Indeed, readers familiar with multi-input multi-output applications of QFT will recognize Eq. (16) as the relation used to define equivalent multi-input single-output problems in that synthesis procedure.

Example

A brief example is in order at this juncture. A lateral/directional stability and command augmentation system (SCAS) is to be designed for a model of the AFTI F-16 fighter aircraft. The model is taken from Ref. 7. The system state-space model is given next where the flight condition is Mach 0.9 at an altitude of 20,000 ft:

$$\begin{Bmatrix} \dot\phi \\ \dot\beta \\ \dot p \\ \dot r \end{Bmatrix} = \begin{bmatrix} 0 & 0 & 1 & 0 \\ 0.0345 & -0.3436 & 0.0326 & -0.9976 \\ 0 & -55.256 & -2.80 & 0.1457 \\ 0 & 7.237 & -0.0232 & -0.3625 \end{bmatrix} \begin{Bmatrix} \phi \\ \beta \\ p \\ r \end{Bmatrix}$$

$$+ \begin{bmatrix} 0 & 0 \\ -.00014 & 0.0373 \\ -51.05 & 10.395 \\ -1.2501 & -5.808 \end{bmatrix} \begin{Bmatrix} \delta_a \\ \delta_r \end{Bmatrix} \tag{17}$$

In Eq. (17), the angles and angular rates are in degrees and degrees per second. Actuator dynamics, have been ignored for simplicity. The system response variables are roll rate p and lateral acceleration of the center of gravity a_y. The corresponding output equations are

$$\begin{Bmatrix} p \\ a_y \end{Bmatrix} = \begin{bmatrix} 0 & 0 & 1 & 0 \\ 0 & -5.596 & 0.5309 & 0.0390 \end{bmatrix} \cdot \begin{Bmatrix} \phi \\ \beta \\ p \\ r \end{Bmatrix}$$

$$+ \begin{bmatrix} 0 & 0 \\ -0.0227 & 0.6075 \end{bmatrix} \cdot \begin{Bmatrix} \delta_a \\ \delta_r \end{Bmatrix} \tag{18}$$

In Eq. (18), the lateral acceleration is in feet per second squared. Transmission zeros of this plant are located at $s = 6.9014, -6.8757$, and 0. The zero at the origin is related to the kinematic relation between roll angle and rate and is not of concern. Note that one transmission zero lies in the RHP.

An examination of both the elements of $P(s)$ and the four possible input–output pairs (with tightly constrained variables in the remaining loop) can be made, with the latter four obtained from Eqs. (8) and (16). When shorthand notation is used,

$$\frac{K(a)}{[\zeta, \omega_n]} = \frac{K(s+a)}{s^2 + 2\zeta\omega_n + \omega_n^2}$$

the transfer functions are

$$\frac{p}{\delta_a} = \frac{-51.05[0.12, 2.949]}{(2.697)(0.0272)[0.131, 2.987]} \tag{19a}$$

$$\frac{p}{\delta_r} = \frac{10.395(5.071)(-4.644)}{(2.697)(0.0272)[0.131, 2.987]} \tag{19b}$$

$$\frac{a_y}{\delta_a} = \frac{-0.2279(1199)(-.01269)[0.108, 2.949]}{(2.697)(0.272)[0.131, 2.987]} \tag{19c}$$

$$\frac{a_y}{\delta_r} = \frac{0.6073(13.2)(4.502)(-5.831)(.002362)}{(2.697)(0.2762)[0.131, 2.987]} \tag{19d}$$

$$\left.\frac{p}{\delta_a}(s)\right|_{a_y \to \delta_r} \cong \frac{-50.66(0)(-6.9014)(6.8757)}{(13.2)(4.502)(-5.831)(0.002366)} \tag{20a}$$

$$\left.\frac{a_y}{\delta_r}(s)\right|_{p \to \delta_a} \cong \frac{0.6029(-6.9014)(6.8757)}{[0.12, 2.949]} \tag{20b}$$

$$\left.\frac{a_y}{\delta_a}(s)\right|_{p \to \delta_r} \cong \frac{-1349.9(0)(-6.9014)(6.8757)}{(1199)(-.01269)[0.108, 2.949]} \tag{20c}$$

$$\left.\frac{p}{\delta_r}(s)\right|_{a_y \to \delta_a} \cong \frac{2.960(-6.9014)(6.8757)}{(5.071)(-4.644)} \tag{20d}$$

Equations (19) and (20) can provide insight into input–output pairing in a sequential loop-closure design. For example, if p is paired with δ_r and this loop is closed first, Eq. (19b) indicates that maintenance of acceptable stability margins would allow a maximum crossover frequency no larger that 1–2 rad/s due to the NMP zero at $s = 4.644$. It is doubtful that this would result in an acceptable bandwidth from the standpoint of handling qualities of a primary attitude axis. If a_y is paired with δ_a, and this loop is closed first, Eq. (19c) indicates that only very small crossover frequencies could be employed because of the zero at $s = 0.01269$.

If p is paired with δ_a and this loop is closed first, Eq. (19a) indicates that arbitrarily large crossover frequencies could be employed. Equation (20b) indicates that closing the a_y loop with δ_r next can be successful with a crossover frequency in the range of 1–2 rad/s due to a NMP zero at $s = 6.9014$. If a_y is paired with δ_r and this loop is closed first, Eq. (19d) indicates the loop would have a maximum crossover frequency in the range of 1–2 rad/s due to the NPM zero at $s = 5.831$. Because of to the limited bandwidth of this first closure,

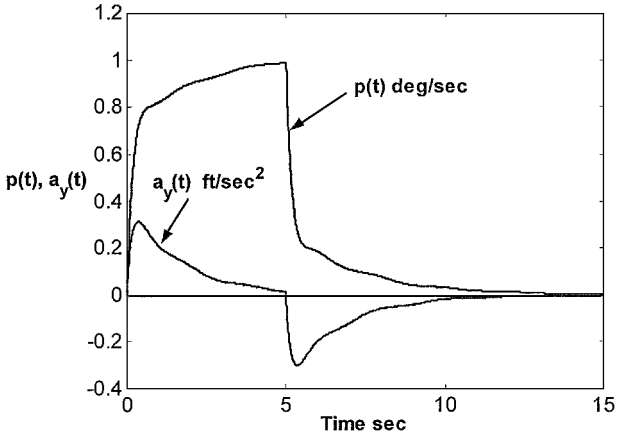

Fig. 2 Response of aircraft to unit pulse roll-rate p command.

the use of Eq. (20a) would not be justified here because one could not assume that a_y is tightly constrained.

This exercise suggests a sequential loop-closure design procedure with the p and a_y variables paired with δ_a and δ_r, respectively, closing the p loop first. Had matrix $K(s)$ in Fig. 1 not been the identity matrix, an analysis similar to that just completed could be undertaken with the transfer functions of Eq. (19) obtained from $P'(s) = P(s)K(s)$ and those of Eq. (20) obtained from relationships such as Eq. (14). In cases in which there are no NMP transmission zeros, pairing input–output variables and selecting loop-closure sequences could be based on the required compensation in each loop. The form of this compensation could be estimated from equations similar to Eqs. (19) and (20).

Figure 1 can serve as a diagram for the SCAS, now with $y_1(s) = p(s)$, $y_2(s) = a_y(s)$, $u_1(s) = \delta_a(s)$, $u_2(s) = \delta_r(s)$, and $K(s) = I$. The compensator $G_1(s)$ in Fig. 1 was obtained using standard loop-shaping techniques.[8] The result was a 5 rad/s open-loop crossover frequency with

$$G_1(s) = \frac{0.074(3)(0.1)^2}{(0)^2(0.2)} \tag{21}$$

The effective plant for the second loop closure [now determined using the actual $G_1(s)$ of Eq. (21)] is given by

$$\left.\frac{a_y}{\delta_r}\right|_{p \to \delta_a} = \frac{0.6075(15.71)(4.833)(-6.11)(1.147)}{[0.962, 3.385][0.131, 2.943]} \tag{22}$$

Because of the NMP zero in the numerator at $s = 6.11$, the maximum practical crossover frequency for this loop with acceptable stability margins is approximately 1 rad/s. Again, a compensator was obtained using standard loop-shaping techniques and is given by

$$G_2(s) = \frac{-1.42[0.15, 3]}{(0)(50)} \tag{23}$$

The response of the aircraft to a 5-s unit pulse command in p with this SCAS is shown in Fig. 2. Similar command following and off-axis responses result when a unit pulse command in a_y is employed.

Conclusions

The use of coupling numerators based on output equations as opposed to state equations results in a simplification of the coupling numerator expressions. The use of these simplified numerators in square control systems with response variables assumed to be tightly constrained provides insight into the selection of appropriate pairings of plant inputs and outputs for square feedback designs. In addition, it demonstrates the effect of transmission zeros on individual effective plant transfer function elements, when other response variables are tightly constrained.

References

[1] McRuer, D., Ashkenas, I., and Graham, D., *Aircraft Dynamics and Automatic Control*, Princeton Univ. Press, Princeton, NJ, 1973, Chap. 3.

[2] Heffley, R. K., "A Compilation and Analysis of Helicopter Handling Qualities Data," NASA CR-3144, March 1979.

[3] Catapang, D. R., Tischler, M. B., and Biezad, D. J., "Robust Crossfeed Design for Hovering Rotorcraft," *International Journal of Control*, Vol. 4, No. 1, 1994, pp. 161–180.

[4] Stengel, R. F., *Stochastic Optimal Control*, Wiley, New York, 1986, p. 544.

[5] Horowitz, I., *Quantitative Feedback Theory*, QFT Publications, Boulder, CO, 1993.

[6] Wells, S. R., and Hess, R. A., "MIMO Sliding Mode Control for a Tailless Fighter Aircraft," *Journal of Guidance, Control, and Dynamics* (to be published).

[7] Rivard, G. R., "Weighting Matrix Selection for QFT Designs," M.S. Thesis, Air Force Inst. of Technology, No. AFIT/GE/ENG/89D-43, Wright–Patterson AFB, OH, Dec. 1989.

[8] Maciejowski, J. M., *Multivariable Feedback Design*, Addison–Wesley, Wokingham, England, U.K., 1989, Chap. 1.

Inverse Solar Sail Trajectory Problem

Colin R. McInnes*
University of Glasgow, Glasgow, Scotland G12 8QQ, United Kingdom

I. Introduction

SOLAR sailing has long been considered for a diverse range of future mission applications. Although low-performance solar sails can be utilized for interplanetary transfer using heliocentric spiral trajectories, high-performance solar sails can enable exotic applications using non-Keplerian orbits. A simple example of such an exotic application is "levitation," with the solar radiation pressure acceleration experienced by the sail exactly balancing solar gravity. Such a static equilibrium allows the solar sail to remain stationary with respect to the sun, or indeed if the sail is turned edgewise to the sun it will fall sunwards on a rectilinear trajectory. Although this static equilibrium is simple to identify, the question of transfer to it from an Earth escape trajectory remains open. This Note will derive an analytic sail steering law that allows the solar sail is be maneuvered from a circular heliocentric orbit, to a static equilibrium location at the same heliocentric distance. The required trajectory will be defined a priori with the resulting sail steering law derived from the equations of motion. An inverse trajectory problem is, therefore, being solved.

II. Static Equilibria

To identify conditions for static equilibria, the equations of motion for the solar sail will now be defined. The heliocentric equations of motion for an ideal, planar solar sail may be written in plane polar coordinates (r, θ) as[1]

$$\ddot{r} - r\dot{\theta}^2 = -(\mu/r^2)(1 - \beta\cos^3\alpha) \tag{1a}$$

$$r\ddot{\theta} + 2\dot{r}\dot{\theta} = \beta(\mu/r^2)\cos^2\alpha\sin\alpha \tag{1b}$$

where r is the heliocentric distance of the solar sail from the sun and θ is the polar angle of the solar sail, measured anticlockwise from some reference position. Because both solar radiation pressure and solar gravity have an inverse square variation, the solar sail performance can be parameterized by the sail lightness number β,

Received 12 February 2002; revision received 12 June 2002; accepted for publication 17 September 2002.

*Professor, Department of Aerospace Engineering; colinmc@aero.gla.ac.uk.